

JAERI-M
86-156

NONLINEAR EVOLUTION OF FREE-BOUNDARY
KINK MODE IN A TOKAMAK

October 1986

Gen-ichi KURITA, Tomonori TAKIZUKA
Masafumi AZUMI and Tatsuoki TAKEDA

JAERI-Mレポートは、日本原子力研究所が不定期に公刊している研究報告書です。
入手の問い合わせは、日本原子力研究所技術情報部情報資料課（〒319-11 茨城県那珂郡東海村）あて、お申しこしください。なお、このほかに財団法人原子力弘済会資料センター（〒319-11 茨城県那珂郡東海村日本原子力研究所内）で複写による実費領布をおこなっております。

JAERI-M reports are issued irregularly.
Inquiries about availability of the reports should be addressed to Information Division Department of Technical Information, Japan Atomic Energy Research Institute, Tokaimura, Naka-gun, Ibaraki-ken 319-11, Japan.

© Japan Atomic Energy Research Institute, 1986

編集兼発行 日本原子力研究所
印 刷 日青工業株式会社

NONLINEAR EVOLUTION OF FREE-BOUNDARY KINK MODE
IN A TOKAMAK

Gen-ichi KURITA, Tomonori TAKIZUKA, Masafumi AZUMI
and Tatsuoki TAKEDA

Department of Thermonuclear Fusion Research
Naka Fusion Research Establishment
Japan Atomic Energy Research Institute
Naka-machi, Naka-gun, Ibaraki-ken

(Received October 3, 1986)

Nonlinear MHD calculations of the $m/n=2/1$ free-boundary kink mode in a cylindrical tokamak are carried out by taking account of the parallel diffusion of resistivity. The "vacuum bubbles" inside the plasma are formed for q_a a little smaller than 2. When $1.75 < q_a < 1.9$ for $q_0/q_a=0.5$ (q_0 is the safety factor at the magnetic axis and q_a is that at the plasma surface), the plasma column shrinks with the elliptic deformation, the value of q_a is decreased in time, the plasma becomes stable against the $m/n=2/1$ mode, and finally damping oscillation is observed. Interaction between the plasma and material limiter causes the shrinkage for all the unstable values of q_a . When q_0 is nearly equal to or larger than unity, the plasma shrinks rapidly and q_a can be reduced less than unity below which the $m/n=1/1$ kink mode becomes unstable. This plasma shrinkage is a candidate of the major disruptions in the tokamak discharge with q_a less or equal to 2.

Keywords; Nonlinear Simulation, Plasma Shrinkage, Free-Boundary Kink Mode,
Major Disruption, Tokamak

トカマクにおける自由境界キンクモードの非線形発展

日本原子力研究所那珂研究所核融合研究部

栗田 源一・滝塚 知典・安積 正史・竹田 辰興

(1986年10月3日受理)

円筒トカマクにおける $m/n = 2/1$ 自由境界キンクモードの非線形計算を、抵抗の磁力線方向拡散を考慮して行なった。2より少し小さい q_a に対してプラズマ内部に“磁気泡”が形成される。 q_0/q_a が 0.5 (q_0 と q_a は各々磁気軸とプラズマ表面での安全係数) に対して、 q_a の値が 1.75 から 1.9 までの時、プラズマ柱は楕円変形しながら収縮し時間とともに q_a の値が下がって、プラズマは $m/n = 2/1$ モードに対して安定となり、最後に減衰振動が観測される。プラズマとリミターの相互作用は、すべての不安定な q_a の値に対して、この収縮を引起す。 q_0 が 1 に等しいか、それより大きい時、プラズマは急激に収縮し、 q_a は 1 より小さくなって、 $m/n = 1/1$ のキンクモードが不安定になる。このプラズマ収縮は q_a が 2 以下のトカマク放電におけるメジャー・ディスラプションの候補の一つである。

CONTENTS

1. INTRODUCTION	1
2. BASIC EQUATIONS	1
3. LINEAR STABILITY ANALYSIS	2
4. NONLINEAR CALCULATIONS	3
4.a Case without limiter	4
4.b Case with limiter	5
4.c Negative surface current	6
5. SUMMARY AND DISCUSSION	7
ACKNOWLEDGMENTS	8
REFERENCES	8
FIGURES	9

目 次

1. はじめに	1
2. 基礎方程式	1
3. 線形安定性解析	2
4. 非線形計算	3
4.a リミターなしの場合	4
4.b リミターありの場合	5
4.c 負の表面電流	6
5. まとめと討論	7
謝 辞	8
参考文献	8
図	9

1. INTRODUCTION

In the tokamak discharges with q_a nearly equal to 2, some major disruptions are observed which limit the maximum plasma current [1,2]. The $m/n=2/1$ tearing mode (m and n are the poloidal and toroidal mode numbers, respectively) is considered to play an important role in this major disruption process. This disruption process has been studied by numerical calculations [3,4,5]. The $m/n=2/1$ free-boundary kink mode is also considered to play an important role in the major disruption. The following scenario has been supposed: The plasma deforms elliptically due to the growth of the kink mode and the deformation is saturated by the negative surface current. With the dissipation of the surface current due to the plasma-limiter interaction, however, the deformation continues to grow and the current disruption is caused [6,7]. In this report, we demonstrate a new scenario of the disruption by means of numerical calculations of the $m/n=2/1$ free-boundary kink mode, where the resistivity evolution including parallel diffusion is considered. In section 2, basic equations are described. The linear stability of free-boundary kink mode including resistivity equation with finite κ_{\parallel} is analysed in section 3. The results of nonlinear evolutions are shown in section 4, and summary and discussion are given in section 5.

2. BASIC EQUATIONS

As basic equations, we employ the single-helicity reduced set of resistive MHD equations of a low beta cylindrical plasma including the resistivity evolution equation:

$$\frac{\partial \Psi_{m/n}}{\partial t} = [\Psi, \Phi]_{m/n} + \sum_{m=m'+m''} \sum_{n=n'+n''} \eta_{m'/n'} J_{m''/n''} - E^v \delta_{m0} \delta_{n0}, \quad (1)$$

$$\frac{\partial U_{m/n}}{\partial t} = [U, \Phi]_{m/n} + [\Psi, J]_{m/n}, \quad (2)$$

$$\frac{\partial \eta_{m/n}}{\partial t} = [\eta, \Phi]_{m/n} - \kappa_{\parallel} [\nabla_{\parallel} \eta, \Psi]_{m/n} + \kappa_{\perp} \Delta \eta_{m/n}, \quad (3)$$

$$U_{m/n} = \Delta \Phi_{m/n}, \quad (4)$$

1. INTRODUCTION

In the tokamak discharges with q_a nearly equal to 2, some major disruptions are observed which limit the maximum plasma current [1,2]. The $m/n=2/1$ tearing mode (m and n are the poloidal and toroidal mode numbers, respectively) is considered to play an important role in this major disruption process. This disruption process has been studied by numerical calculations [3,4,5]. The $m/n=2/1$ free-boundary kink mode is also considered to play an important role in the major disruption. The following scenario has been supposed: The plasma deforms elliptically due to the growth of the kink mode and the deformation is saturated by the negative surface current. With the dissipation of the surface current due to the plasma-limiter interaction, however, the deformation continues to grow and the current disruption is caused [6,7]. In this report, we demonstrate a new scenario of the disruption by means of numerical calculations of the $m/n=2/1$ free-boundary kink mode, where the resistivity evolution including parallel diffusion is considered. In section 2, basic equations are described. The linear stability of free-boundary kink mode including resistivity equation with finite κ_{\parallel} is analysed in section 3. The results of nonlinear evolutions are shown in section 4, and summary and discussion are given in section 5.

2. BASIC EQUATIONS

As basic equations, we employ the single-helicity reduced set of resistive MHD equations of a low beta cylindrical plasma including the resistivity evolution equation:

$$\frac{\partial \Psi_{m/n}}{\partial t} = [\Psi, \Phi]_{m/n} + \sum_{m=m'+m''} \sum_{n=n'+n''} \eta_{m'/n'} J_{m''/n''} - E^v \delta_{m0} \delta_{n0}, \quad (1)$$

$$\frac{\partial U_{m/n}}{\partial t} = [U, \Phi]_{m/n} + [\Psi, J]_{m/n}, \quad (2)$$

$$\frac{\partial \eta_{m/n}}{\partial t} = [\eta, \Phi]_{m/n} - \kappa_{\parallel} [\nabla_{\parallel} \eta, \Psi]_{m/n} + \kappa_{\perp} \Delta \eta_{m/n}, \quad (3)$$

$$U_{m/n} = \Delta \Phi_{m/n}, \quad (4)$$

$$J_{m/n} = \Delta \Psi_{m/n} , \quad (5)$$

$$[X, Y]_{m/n} \equiv \sum_{m=m'+m''} \sum_{n=n'+n''} \frac{m'}{r} (X_{m'/n'} \frac{\partial Y_{m''/n''}}{\partial r} - Y_{m'/n'} \frac{\partial X_{m''/n''}}{\partial r}) , \quad (6)$$

where $\Psi_{m/n}$ is the helical poloidal magnetic flux, $\Phi_{m/n}$ the stream function, $\eta_{m/n}$ the resistivity, $J_{m/n}$ the current density, $U_{m/n}$ the vorticity, E^w the electric field at the wall, and δ_{ij} is the Kronecker's delta. In these equations, the uniform plasma density is assumed, and the time is normalized by the poloidal Alfvén transit time $\tau_{p\alpha} = B_t / \sqrt{\rho} R$ (B_t is the toroidal magnetic field, ρ the plasma density, and R the major radius). Other normalization factors are $\sqrt{\rho} R / (B_t b^2)$ for η and $\sqrt{\rho} R / (B_t R^2)$ for κ_{\parallel} .

The resistivity is assumed to follow the same equation as that for the electron temperature. The parallel diffusion coefficient of resistivity, κ_{\parallel} , and perpendicular one, κ_{\perp} , are assumed to be uniform for simplicity. The parallel gradient of η is defined as $(\nabla_{\parallel} \eta)_{m/n} = [\eta, \Psi]_{m/n}$. To calculate the free-boundary problem, we use the "pseudo-vacuum" model, where the vacuum is replaced by the plasma with high resistivity. This method has been successfully applied to nonlinear simulations of free-boundary modes [8,9]. The above set of nonlinear equations is solved by the predictor-corrector time integration scheme. The diffusion terms in eqs.(1) and (3) are approximated by the implicit representation. These implicit parts of nonlinear calculation spend almost CPU time of the computer. The equation for resistivity, eq.(3), including the diffusion term is solved by a mapping method which is described in ref. [8].

3. LINEAR STABILITY ANALYSIS

In this section, we investigate the effect of parallel diffusion on the linear stability of free-boundary kink mode. From eqs.(1)~(6), the following linearized reduced set of resistive MHD equations is derived,

$$\gamma \Delta \Phi = F \Delta \Psi - \frac{m dJ_{eq}}{r dr} \Psi , \quad (7)$$

$$\gamma \Psi = -F \Phi + \eta_{eq} \Delta \Psi + \eta J_{eq} , \quad (8)$$

$$J_{m/n} = \Delta \Psi_{m/n} , \quad (5)$$

$$[X, Y]_{m/n} \equiv \sum_{m=m'+m''} \sum_{n=n'+n''} \frac{m'}{r} (X_{m'/n'} \frac{\partial Y_{m''/n''}}{\partial r} - Y_{m'/n'} \frac{\partial X_{m''/n''}}{\partial r}) , \quad (6)$$

where $\Psi_{m/n}$ is the helical poloidal magnetic flux, $\Phi_{m/n}$ the stream function, $\eta_{m/n}$ the resistivity, $J_{m/n}$ the current density, $U_{m/n}$ the vorticity, E^w the electric field at the wall, and δ_{ij} is the Kronecker's delta. In these equations, the uniform plasma density is assumed, and the time is normalized by the poloidal Alfvén transit time $\tau_{pa} = B_t / \sqrt{\rho} R$ (B_t is the toroidal magnetic field, ρ the plasma density, and R the major radius). Other normalization factors are $\sqrt{\rho} R / (B_t b^2)$ for η and $\sqrt{\rho} R / (B_t R^2)$ for κ_{\parallel} .

The resistivity is assumed to follow the same equation as that for the electron temperature. The parallel diffusion coefficient of resistivity, κ_{\parallel} , and perpendicular one, κ_{\perp} , are assumed to be uniform for simplicity. The parallel gradient of η is defined as $(\nabla_{\parallel} \eta)_{m/n} = [\eta, \Psi]_{m/n}$. To calculate the free-boundary problem, we use the "pseudo-vacuum" model, where the vacuum is replaced by the plasma with high resistivity. This method has been successfully applied to nonlinear simulations of free-boundary modes [8,9]. The above set of nonlinear equations is solved by the predictor-corrector time integration scheme. The diffusion terms in eqs.(1) and (3) are approximated by the implicit representation. These implicit parts of nonlinear calculation spend almost CPU time of the computer. The equation for resistivity, eq.(3), including the diffusion term is solved by a mapping method which is described in ref. [8].

3. LINEAR STABILITY ANALYSIS

In this section, we investigate the effect of parallel diffusion on the linear stability of free-boundary kink mode. From eqs.(1)~(6), the following linearized reduced set of resistive MHD equations is derived,

$$\gamma \Delta \Phi = F \Delta \Psi - \frac{m d J_{eq} \Psi}{r dr} , \quad (7)$$

$$\gamma \Psi = -F \Phi + \eta_{eq} \Delta \Psi + \eta J_{eq} , \quad (8)$$

$$\gamma\eta = - \frac{m d\eta_{eq}}{r dr} \Phi + \kappa_{\parallel} F \left(\frac{m d\eta_{eq}}{r dr} \Psi - F\eta \right), \quad (9)$$

$$F = \frac{1}{q} (m-nq), \quad (10)$$

where q is the safety factor, subscript "eq" means equilibrium quantities, and the time derivatives are replaced by the growth rate, γ . The perpendicular diffusion is negligibly small in general. Since the singular surface ($F=0$) does not exist in the plasma region for the kink mode ($q_a < m/n$), $\gamma\Psi \approx -F\Phi$ holds and eq.(9) becomes

$$\left(1 + \frac{\kappa_{\parallel} F^2}{\gamma} \right) \left(\gamma\eta + \frac{m d\eta_{eq}}{r dr} \Phi \right) \approx 0. \quad (11)$$

This relation implies that the parallel diffusion scarcely affects the kink mode in the linear stage. Numerical calculations of the eigenvalue problem support above prediction. Figure 1 shows the linear growth rates of $m/n=2/1$ free-boundary kink mode versus q_a for various values of κ_{\parallel} . The ratio of the plasma radius, a , to the wall radius, b , is $a/b=0.66$. The resistivity, $\eta_{eq}(r)$, is inversely proportional to $J_{eq}(r)$ with $\eta_{eq}(0)=10^{-5}$ and $\eta_{eq}(b)=1$. The profile of current density is chosen as

$$J_{eq}(r) = \{ J_{eq}(0) - J_{eq}(b) \} \{ 1 - (r/a)^{3.56} \}^2 + J_{eq}(b), \quad (12)$$

for $0 \leq r \leq a$, and $J_{eq}(r) = J_{eq}(b) = J_{eq}(0)\eta_{eq}(0)/\eta_{eq}(b)$ for $a < r \leq b$. The ratio, q_0/q_a , is 0.5 for this current profile, and the value of $J_{eq}(0)$ is determined by the value of q_0 . The relatively large value of the linear growth rate at $q_a \approx 2.0$ is attributed to the finite plasma resistivity near the singular surface and the growth rate of the kink mode is smoothly connected to that of the "surface tearing mode" in the $q_a > 2.0$ region [10]. The parallel diffusion of resistivity becomes very important in the nonlinear phase, especially in the phase of the interaction between plasma and limiter.

4. NONLINEAR CALCULATIONS

In this section, we carry out nonlinear calculations of the $m/n=2/1$ free-boundary kink mode for the cases (4.a) without a limiter and (4.b) with a limiter. The initial profile of current density is given by

$$\gamma\eta = -\frac{m}{r}\frac{d\eta_{eq}}{dr}\Phi + \kappa_{\parallel}F\left(\frac{m}{r}\frac{d\eta_{eq}}{dr}\Psi - F\eta\right), \quad (9)$$

$$F = \frac{1}{q}(m-nq), \quad (10)$$

where q is the safety factor, subscript "eq" means equilibrium quantities, and the time derivatives are replaced by the growth rate, γ . The perpendicular diffusion is negligibly small in general. Since the singular surface ($F=0$) does not exist in the plasma region for the kink mode ($q_a < m/n$), $\gamma\Psi \approx -F\Phi$ holds and eq.(9) becomes

$$\left(1 + \frac{\kappa_{\parallel}F^2}{\gamma}\right)\left(\gamma\eta + \frac{m}{r}\frac{d\eta_{eq}}{dr}\Phi\right) \approx 0. \quad (11)$$

This relation implies that the parallel diffusion scarcely affects the kink mode in the linear stage. Numerical calculations of the eigenvalue problem support above prediction. Figure 1 shows the linear growth rates of $m/n=2/1$ free-boundary kink mode versus q_a for various values of κ_{\parallel} . The ratio of the plasma radius, a , to the wall radius, b , is $a/b=0.66$. The resistivity, $\eta_{eq}(r)$, is inversely proportional to $J_{eq}(r)$ with $\eta_{eq}(0)=10^{-6}$ and $\eta_{eq}(b)=1$. The profile of current density is chosen as

$$J_{eq}(r) = \{J_{eq}(0) - J_{eq}(b)\} \{1 - (r/a)^{3.56}\}^2 + J_{eq}(b), \quad (12)$$

for $0 \leq r \leq a$, and $J_{eq}(r) = J_{eq}(b) = J_{eq}(0)\eta_{eq}(0)/\eta_{eq}(b)$ for $a < r \leq b$. The ratio, q_0/q_a , is 0.5 for this current profile, and the value of $J_{eq}(0)$ is determined by the value of q_0 . The relatively large value of the linear growth rate at $q_a \approx 2.0$ is attributed to the finite plasma resistivity near the singular surface and the growth rate of the kink mode is smoothly connected to that of the "surface tearing mode" in the $q_a > 2.0$ region [10]. The parallel diffusion of resistivity becomes very important in the nonlinear phase, especially in the phase of the interaction between plasma and limiter.

4. NONLINEAR CALCULATIONS

In this section, we carry out nonlinear calculations of the $m/n=2/1$ free-boundary kink mode for the cases (4.a) without a limiter and (4.b) with a limiter. The initial profile of current density is given by

eq. (12) ($q_0/q_a|_{t=0}=0.5$) except the calculation for Fig.4 (initial values of q_a and q_0 are 1.85 and 1.2, respectively). Total plasma current is assumed to be constant in time. The resistivity at $t=0$ is determined as $\eta(r)=E^w/J(r)$ with $\eta(0)=10^{-6}$ and $\eta(b)=1$. We choose, in the following calculations, the initial plasma radius, a_0 , as $a_0/b=0.66$. The parallel diffusion coefficient, κ_{\parallel} is set 10^2 , and $\kappa_{\perp}=10^{-8}$. The nonuniformity of η on a magnetic surface disappears within the time interval of about 0.1 due to the diffusion of $\kappa_{\parallel}=10^2$. This value of κ_{\parallel} corresponds to the following actual parameters; toroidal magnetic field $B_t=4$ T, major radius $R=1$ m, electron temperature $T_e=1$ keV, and plasma density $n=10^{20}$ m $^{-3}$. Number of Fourier components, M , and radial meshes, N_r , are typically $M=10$ and $N_r=200$.

4.a Case without limiter

The nonlinear evolutions without limiter are studied at first for various initial values of $q_{a0}=q_a(t=0)$; (a) $q_{a0}=1.75$, (b) $q_{a0}=1.8$, (c) $q_{a0}=1.85$, (d) $q_{a0}=1.9$, (e) $q_{a0}=1.95$ and (f) $q_{a0}=2.0$. Figures 2 and 3 show the time evolutions of Ψ -contour for $q_{a0}=1.85$ and $q_{a0}=1.95$, respectively. The bold line in the figure represents crowded resistivity contours which correspond to the approximate position of the plasma surface. For $q_{a0}=1.85$, the elliptic deformation grows with the shrinkage of the plasma column ($0 < t < 112.5$). Since the plasma current is constant, this shrinkage makes q_a value small from 1.85 to 1.25, and the plasma becomes linearly stable against the $m/n=2/1$ kink mode. Finally the damping oscillation of the shrunk plasma is observed ($t > 112.5$). The shrinkage of the plasma column is caused by the following processes. An η -contour in a resistive plasma crosses Ψ -contours near the plasma surface due to the convection, and the plasma periphery connected with the vacuum region is drastically cooled by the parallel thermal conduction. It is to be noted for the case of $\kappa_{\parallel}=0$ that the plasma area is conserved and the saturation state with elliptic deformation can be realized [8]. On the other hand, for larger q_{a0} value ($q_{a0}=1.95$), the "vacuum bubble" is formed by the free-boundary kink mode, as shown in Fig.3, even for such a decreasing current profile ($q_0/q_a|_{t=0}=0.5$). The hot plasma flows out into the "pseudo-vacuum" region along the magnetic field line and the vacuum region penetrates into the plasma to form the "vacuum bubbles". It was shown by

Rosenbluth et al. that the saturation state of the ideal kink mode is the elliptic deformation for the parabolic current profile [11]. The "vacuum bubble" was found to be formed by the surface tearing mode in a resistive plasma for $q_{a0} > 2$ and $q_0/q_a|_{t=0} = 0.5$ [8]. The bubble formation by the free-boundary kink mode for the initial condition of $q_a = 1.85$ and $q_0 = 1.2$ has been found by Dnestrovskii et al. using the "heating" model for the transport of η in which the convection of plasma boundary is not considered [9]. We perform the calculation for the same initial values of q_a and q_0 as theirs (the initial current profile, $J(r) = J(0)\{1 - (r/a)^{6.14}\}^2$, is different from theirs), and observe the "vacuum bubble" larger than theirs (See Fig.4). This difference may come from the models for the transport of η .

Figure 5 shows cross-sectional shapes of final stage of evolution for various q_{a0} values with the same current profile of eq.(12); (a-c) shrunk plasmas with elliptic deformation and damping oscillation, and (d-f) plasmas with bubbles. The radius of each shrunk plasma with circular cross section is $0.95a_0$ for (a), $0.85a_0$ for (b), and $0.80a_0$ for (c). The transition from the formation of "vacuum bubble" to the shrinkage with elliptic deformation occurs between the q_{a0} values of 1.85 and 1.90 for this current profile. The current profile determines this transition point, but the detailed mechanism or the criterion of this transition is not clarified yet.

4.b Case with limiter

In this subsection, the effect of the limiter on the nonlinear evolution is studied. We assume, for simplicity, that the plasma is surrounded by the limiter for all poloidal and toroidal angles. The limiter radius, b_l , is chosen as $b_l/a_0 = 1.03$ for all cases. The value of κ_{\perp} in the plasma region is 10^{-8} , while that in the vacuum region is set 10^{-4} for numerical reasons. Other parameters are the same as those for the case without the limiter.

Figure 6 shows the time evolution of Ψ -contour for $q_{a0} = 1.85$, where a row of small rectangles denotes the limiter position. After the plasma surface touches the limiter ($t > 55$) the plasma is shrinking as the ellipticity is increasing. When the plasma becomes stable against the $m/n=2/1$ mode at $t \approx 87$, the plasma is detached from the limiter and the

damping oscillation begins. Figure 7 shows the time evolution of magnetic energy of each mode, where the damping oscillation of magnetic energy is observed after the plasma is detached from the limiter ($t > 87$). The mechanism of this phenomenon is essentially the same as the phenomena without limiter for $q_{a0} < 1.9$. In Fig.8 (a), the time evolutions of q_a and the internal inductance, l_i , for the cases with (solid line) and without (broken line) the limiter are shown, where $l_i = \int_S (\vec{\nabla}\Psi)^2 dS / (\vec{\nabla}\Psi)_a^2 S$ (S is the plasma area and a denotes the plasma surface) and its initial value is 1. The final value of q_a is about 1.3 and that of l_i is about 0.7, respectively, for both cases with and without the limiter. In the shrinkage phase with the constant total current, the values of q_0 is unchanged in contrast with the decrease of q_a value, the positive skin current flows near the plasma surface, and the value of l_i becomes small.

The calculation results for the plasma with higher q_{a0} values, i.e. $q_{a0} = 1.95 \sim 2.0$, are much interesting. The phenomena are quite different from the results without the limiter. Since the separatrix always crosses the limiter, the "vacuum bubble" cannot be formed and plasma periphery is cooled as the same as the case of $q_{a0} = 1.85$. The time evolution of q_a value for $q_{a0} = 1.95$ is shown in Fig.8 (b), where the solid curve denotes the case with the limiter and the broken curve denotes the case without the limiter. The q_a value in the saturation state without the limiter is a little higher than initial value, while it becomes nearly equal to 1 for the case with limiter. It should be noted, however, that the numerical results here are obtained from the single-helicity calculations, and in an actual plasma with q_a less than unity, the most dangerous $m/n=1/1$ free-boundary kink mode becomes unstable, which can easily lead the current disruption.

4.c Negative surface current

Figure 9 shows the time evolution of the maximum value of negative surface current near top or bottom of plasma poloidal plane in Fig.6. This is the same calculation as in Fig.8 (b), that is, q_{a0} is chosen as 1.95. The negative surface current developed to suppress the instability does not disappear in spite of the interaction between the plasma and limiter, but even grows rapidly during the contact and disappears suddenly when the plasma reaches the stable state and is detached from the limiter.

This fact is different from the prediction of Kadomtsev [6] or Zakharov [7], but it is plausible that this negative surface current is required to stop the plasma motion at the limiter position while it is unstable state. Almost the same result is obtained for $q_{a0}=2.0$.

5. SUMMARY AND DISCUSSION

The final states of nonlinear $m/n=2/1$ free-boundary kink mode evolution without the limiter are classified into two cases, i.e., the stable state of shrunk plasma and the saturation due to formation of "vacuum bubbles". When the plasma is surrounded by the limiter placed near the plasma surface, the plasma shrinks and goes into the stable state for all the unstable values of q_{a0} ($1.75 < q_{a0} < 2$) for $q_0/q_a|_{t=0}=0.5$. Figure 10 is the stability diagram in the $(q_a, q_0/q_a)$ plane for approximated current profile to that realized in the nonlinear calculations with the limiter, where the hatched region denotes the unstable one. The trajectories of $q_0=\text{const.}$ for $q_{a0}=1.85$ and $q_{a0}=1.95$ are also depicted, which correspond to the results of nonlinear calculations. In this stability calculation, the plasma radius is determined from the condition of constant total current, that is, $a=a_0\sqrt{q_a/q_{a0}}$ with $a_0/b=0.66$. It is easily seen from the figure that higher q_{a0} values for the same q_0/q_a value result in lower q_a value in the final stable state. Final q_a values of nonlinear calculations for both q_{a0} cases are shown in the figure by open squares. In fig.11, we show the calculated linear growth rates versus q_a for $q_{a0}=1.90$ with constant q_0 , unstable region of which is shown in Fig.10. As q_a decreases with decreases of plasma radius, a , and internal inductance, l_i , the linear growth rate increases once and decreases suddenly leading the plasma to be stable state. This is consistent with the energy evolution of $m/n=2/1$ mode for $q_{a0}=1.85$ shown in Fig.7. Because of its inertial effect, the final q_a values decrease lower than the marginally stable values. When the value of q_a becomes near or less equal to one, the most dangerous $m/n=1/1$ free-boundary kink mode becomes unstable and causes the major disruption easily.

It can be concluded that the condition, $q_0 < 1$, is required to pass the dangerous zone of $q_a \approx 2$ in tokamak discharges, because, by the interaction with the limiter, q_a decreases nearly equal to 1 for $q_0 > 1$ and the $m/n=1/1$

This fact is different from the prediction of Kadomtsev [6] or Zakharov [7], but it is plausible that this negative surface current is required to stop the plasma motion at the limiter position while it is unstable state. Almost the same result is obtained for $q_{a0}=2.0$.

5. SUMMARY AND DISCUSSION

The final states of nonlinear $m/n=2/1$ free-boundary kink mode evolution without the limiter are classified into two cases, i.e., the stable state of shrunk plasma and the saturation due to formation of "vacuum bubbles". When the plasma is surrounded by the limiter placed near the plasma surface, the plasma shrinks and goes into the stable state for all the unstable values of q_{a0} ($1.75 < q_{a0} < 2$) for $q_0/q_a|_{t=0}=0.5$. Figure 10 is the stability diagram in the $(q_a, q_0/q_a)$ plane for approximated current profile to that realized in the nonlinear calculations with the limiter, where the hatched region denotes the unstable one. The trajectories of $q_0=\text{const.}$ for $q_{a0}=1.85$ and $q_{a0}=1.95$ are also depicted, which correspond to the results of nonlinear calculations. In this stability calculation, the plasma radius is determined from the condition of constant total current, that is, $a=a_0\sqrt{q_a/q_{a0}}$ with $a_0/b=0.66$. It is easily seen from the figure that higher q_{a0} values for the same q_0/q_a value result in lower q_a value in the final stable state. Final q_a values of nonlinear calculations for both q_{a0} cases are shown in the figure by open squares. In fig.11, we show the calculated linear growth rates versus q_a for $q_{a0}=1.90$ with constant q_0 , unstable region of which is shown in Fig.10. As q_a decreases with decreases of plasma radius, a , and internal inductance, l_i , the linear growth rate increases once and decreases suddenly leading the plasma to be stable state. This is consistent with the energy evolution of $m/n=2/1$ mode for $q_{a0}=1.85$ shown in Fig.7. Because of its inertial effect, the final q_a values decrease lower than the marginally stable values. When the value of q_a becomes near or less equal to one, the most dangerous $m/n=1/1$ free-boundary kink mode becomes unstable and causes the major disruption easily.

It can be concluded that the condition, $q_0 < 1$, is required to pass the dangerous zone of $q_a \approx 2$ in tokamak discharges, because, by the interaction with the limiter, q_a decreases nearly equal to 1 for $q_0 > 1$ and the $m/n=1/1$

kink mode is destabilized (this boundary is shown by a dotted line in Fig.10). The condition of $q_0 < 1$ for realization of low q_a ($q_a < 1.5$) discharges is the same as that in Ref. [9], but the mechanisms are completely different each other. The calculations for the plasma with $q_{a0} > 2$ and dependency of the nonlinear behavior on $\kappa_{||}$ are now being carried out and the complete results of nonlinear $m/n=2/1$ free-boundary mode including the "surface tearing mode" [8,10] will be presented elsewhere.

ACKNOWLEDGMENTS

The authors would like to express their sincere thanks to Drs. T. Tuda and M. Tanaka for their fruitful discussions and continuing encouragements.

REFERENCES

- [1] TOI, K., ITOH, S., KADOTA, K., KAWAHATA, K., NODA, N., SAKURAI, K., SATO, K., TANAHASHI, S., YASUE, S., Nucl. Fusion **19** (1979) 1643.
- [2] NAGAMI, M., YOSHIDA, H., SHINYA, K., JAHNS, G.L., YOKOMIZO, H., SHIMADA, M., IOKI, K., IZUMI, S., KITSUNEZAKI, A., Nucl. Fusion **22** (1982) 409.
- [3] WADDELL, B.V., CARRERAS, B., HICKS, H.R., HOLMES, J.A., LEE, D.K., Phys. Rev. Lett. **41** (1978) 1368; WADDELL, B.V., CARRERAS, B., HICKS, H.R., HOLMES, J.A., Phys. Fluids **22** (1979) 896.
- [4] SYKES, A., WESSON, J.A., Phys. Rev. Lett. **44** (1980) 1215.
- [5] BONDESON, A., Nucl. Fusion **26** (1986) 929.
- [6] KADOMTSEV, B.B., POGUTSE, O.P., Sov. Phys. JETP **38** (1974) 283.
- [7] ZAKHAROV, L.E., Sov. Phys. JETP Lett. **31** (1981) 714.
- [8] KURITA, G., AZUMI, M., TAKIZUKA, T., TUDA, T., TSUNEMATSU, T., TANAKA, Y., TAKEDA, T., Nucl. Fusion **26** (1986) 449.
- [9] DNESTROVSKII, Yu.N., KOSTOMAROV, D.P., POPOV, A.M., SHAGIROV, E.A., Sov. J. Plasma Phys. **11** (1985) 616.
- [10] TAKIZUKA, T., KURITA, G., AZUMI, M., TAKEDA, T., Surface Tearing Modes in Tokamaks, JAERI-M 85-156 (Oct. 1985).
- [11] ROSENBLUTH, M.N., MONTICELLO, D.A., STRAUSS, H.R., WHITE, R.B., Phys. Fluids **19** (1976) 1987.

kink mode is destabilized (this boundary is shown by a dotted line in Fig.10). The condition of $q_0 < 1$ for realization of low q_a ($q_a < 1.5$) discharges is the same as that in Ref. [9], but the mechanisms are completely different each other. The calculations for the plasma with $q_{a0} > 2$ and dependency of the nonlinear behavior on $\kappa_{||}$ are now being carried out and the complete results of nonlinear $m/n=2/1$ free-boundary mode including the "surface tearing mode" [8,10] will be presented elsewhere.

ACKNOWLEDGMENTS

The authors would like to express their sincere thanks to Drs. T. Tuda and M. Tanaka for their fruitful discussions and continuing encouragements.

REFERENCES

- [1] TOI, K., ITOH, S., KADOTA, K., KAWAHATA, K., NODA, N., SAKURAI, K., SATO, K., TANAHASHI, S., YASUE, S., Nucl. Fusion **19** (1979) 1643.
- [2] NAGAMI, M., YOSHIDA, H., SHINYA, K., JAHNS, G.L., YOKOMIZO, H., SHIMADA, M., IOKI, K., IZUMI, S., KITSUNEZAKI, A., Nucl. Fusion **22** (1982) 409.
- [3] WADDELL, B.V., CARRERAS, B., HICKS, H.R., HOLMES, J.A., LEE, D.K., Phys. Rev. Lett. **41** (1978) 1368; WADDELL, B.V., CARRERAS, B., HICKS, H.R., HOLMES, J.A., Phys. Fluids **22** (1979) 896.
- [4] SYKES, A., WESSON, J.A., Phys. Rev. Lett. **44** (1980) 1215.
- [5] BONDESON, A., Nucl. Fusion **26** (1986) 929.
- [6] KADOMTSEV, B.B., POGUTSE, O.P., Sov. Phys. JETP **38** (1974) 283.
- [7] ZAKHAROV, L.E., Sov. Phys. JETP Lett. **31** (1981) 714.
- [8] KURITA, G., AZUMI, M., TAKIZUKA, T., TUDA, T., TSUNEMATSU, T., TANAKA, Y., TAKEDA, T., Nucl. Fusion **26** (1986) 449.
- [9] DNESTROVSKII, Yu.N., KOSTOMAROV, D.P., POPOV, A.M., SHAGIROV, E.A., Sov. J. Plasma Phys. **11** (1985) 616.
- [10] TAKIZUKA, T., KURITA, G., AZUMI, M., TAKEDA, T., Surface Tearing Modes in Tokamaks, JAERI-M 85-156 (Oct. 1985).
- [11] ROSENBLUTH, M.N., MONTICELLO, D.A., STRAUSS, H.R., WHITE, R.B., Phys. Fluids **19** (1976) 1987.

kink mode is destabilized (this boundary is shown by a dotted line in Fig.10). The condition of $q_0 < 1$ for realization of low q_a ($q_a \lesssim 1.5$) discharges is the same as that in Ref. [9], but the mechanisms are completely different each other. The calculations for the plasma with $q_{a0} > 2$ and dependency of the nonlinear behavior on $\kappa_{||}$ are now being carried out and the complete results of nonlinear $m/n=2/1$ free-boundary mode including the "surface tearing mode" [8,10] will be presented elsewhere.

ACKNOWLEDGMENTS

The authors would like to express their sincere thanks to Drs. T. Tuda and M. Tanaka for their fruitful discussions and continuing encouragements.

REFERENCES

- [1] TOI, K., ITOH, S., KADOTA, K., KAWAHATA, K., NODA, N., SAKURAI, K., SATO, K., TANAHASHI, S., YASUE, S., Nucl. Fusion **19** (1979) 1643.
- [2] NAGAMI, M., YOSHIDA, H., SHINYA, K., JAHNS, G.L., YOKOMIZO, H., SHIMADA, M., IOKI, K., IZUMI, S., KITSUNEZAKI, A., Nucl. Fusion **22** (1982) 409.
- [3] WADDELL, B.V., CARRERAS, B., HICKS, H.R., HOLMES, J.A., LEE, D.K., Phys. Rev. Lett. **41** (1978) 1368; WADDELL, B.V., CARRERAS, B., HICKS, H.R., HOLMES, J.A., Phys. Fluids **22** (1979) 896.
- [4] SYKES, A., WESSON, J.A., Phys. Rev. Lett. **44** (1980) 1215.
- [5] BONDESON, A., Nucl. Fusion **26** (1986) 929.
- [6] KADOMTSEV, B.B., POGUTSE, O.P., Sov. Phys. JETP **38** (1974) 283.
- [7] ZAKHAROV, L.E., Sov. Phys. JETP Lett. **31** (1981) 714.
- [8] KURITA, G., AZUMI, M., TAKIZUKA, T., TUDA, T., TSUNEMATSU, T., TANAKA, Y., TAKEDA, T., Nucl. Fusion **26** (1986) 449.
- [9] DNESTROVSKII, Yu.N., KOSTOMAROV, D.P., POPOV, A.M., SHAGIROV, E.A., Sov. J. Plasma Phys. **11** (1985) 616.
- [10] TAKIZUKA, T., KURITA, G., AZUMI, M., TAKEDA, T., Surface Tearing Modes in Tokamaks, JAERI-M 85-156 (Oct. 1985).
- [11] ROSENBLUTH, M.N., MONTICELLO, D.A., STRAUSS, H.R., WHITE, R.B., Phys. Fluids **19** (1976) 1987.

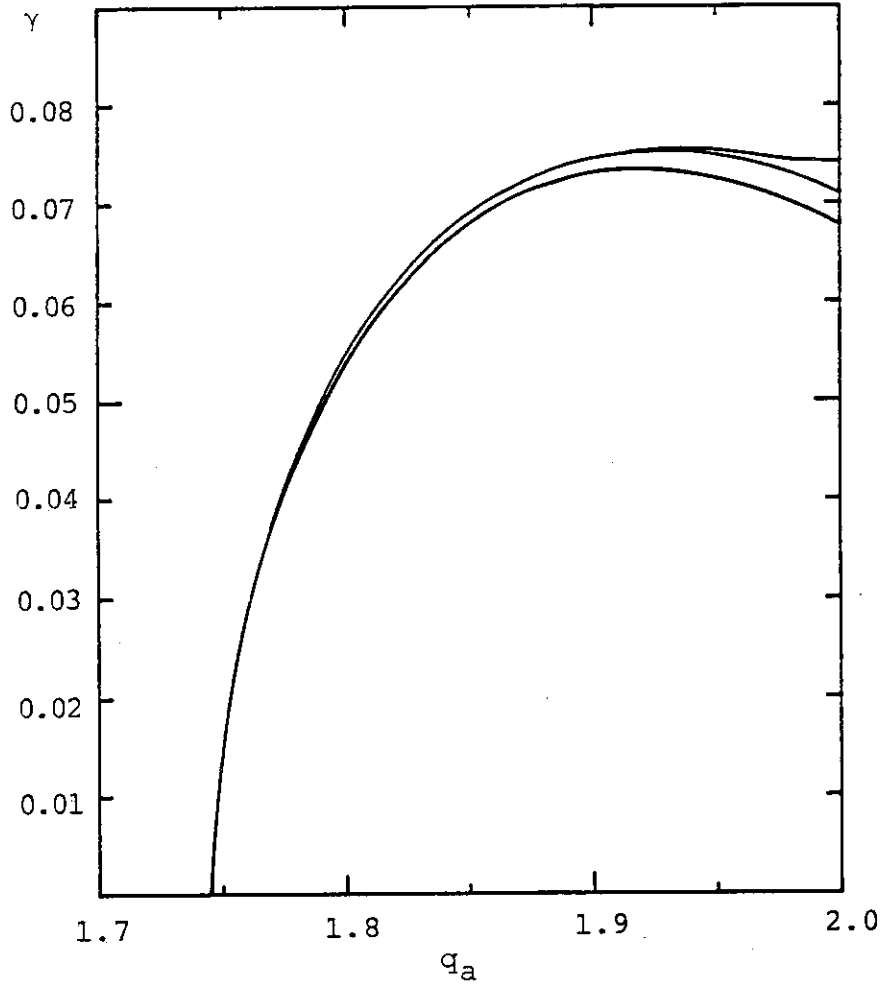


FIG.1 Linear growth rate, γ , versus safety factor at the plasma surface q_a for various values of parallel resistivity diffusion coefficients $\kappa_{||}$ for current profile; $J(r)=J(0)(1-(r/a)^{3.56})^2$. Parameters are chosen as $a/b=0.66$ and $\eta(b)/\eta(0)=10^6$. Values of $\kappa_{||}$ are $10^5, 10^2$ and 10^0 from top to bottom, respectively.

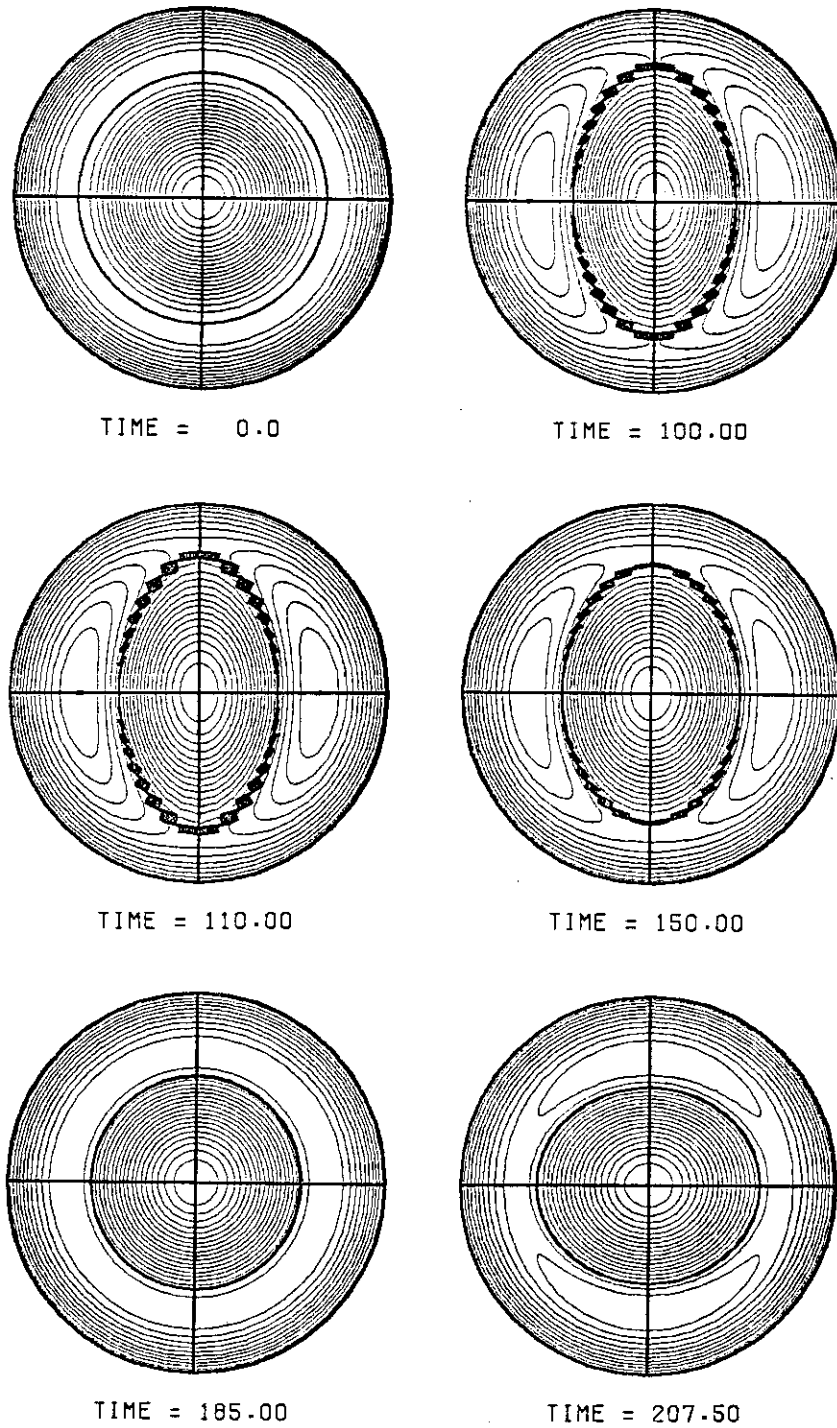


FIG.2 Time evolutions of ψ -contours and plasma surface (bold line) for current profile, $J(r)=J(0)(1-(r/a)^{3.56})^2$, with $q_{a0}=1.85$. Plasma shrinks after elliptic deformation.

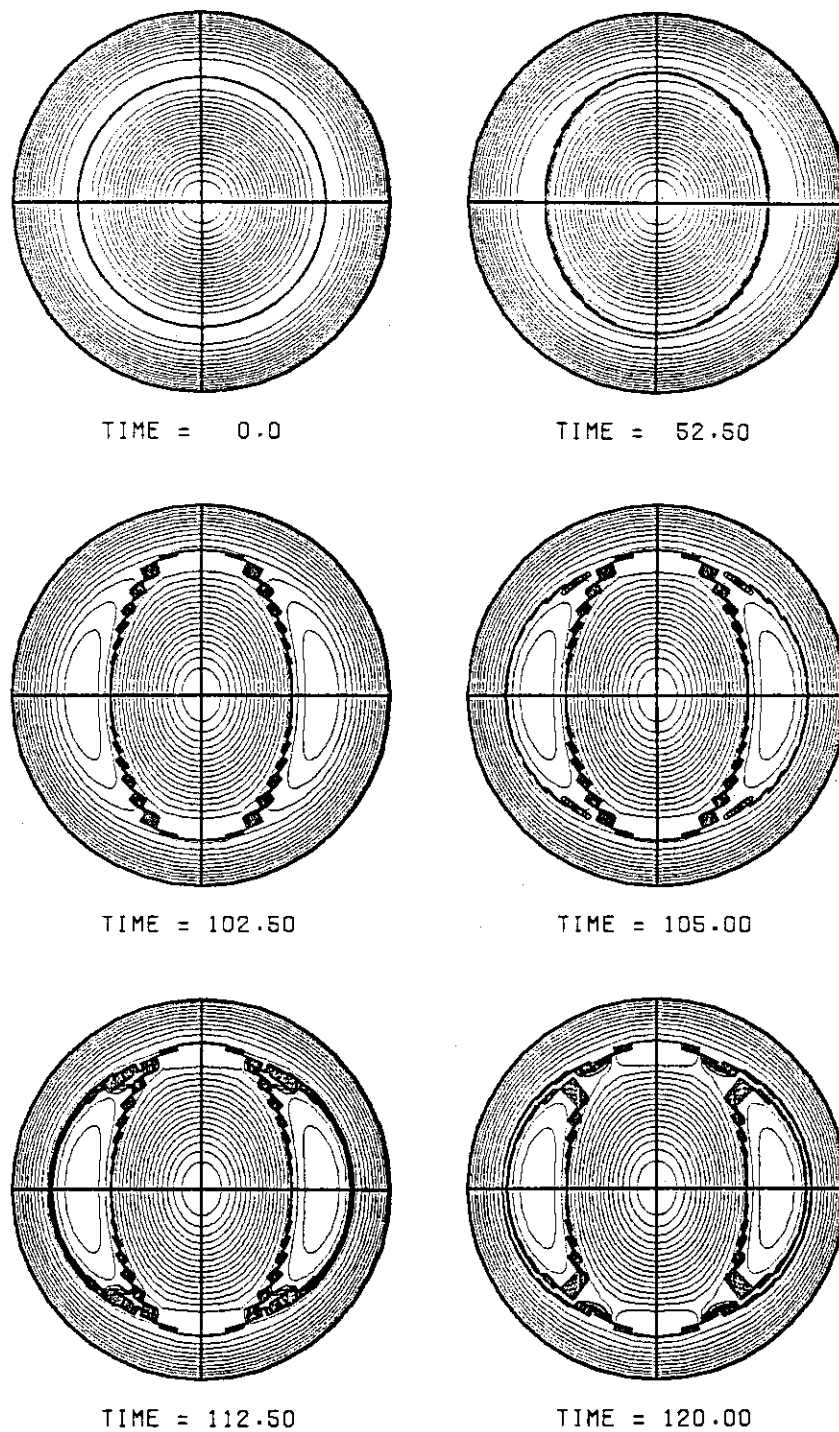


FIG.3 Time evolutions of ψ -contours and plasma surface for $q_{a0}=1.95$. Formation of large "vacuum bubbles" is observed.

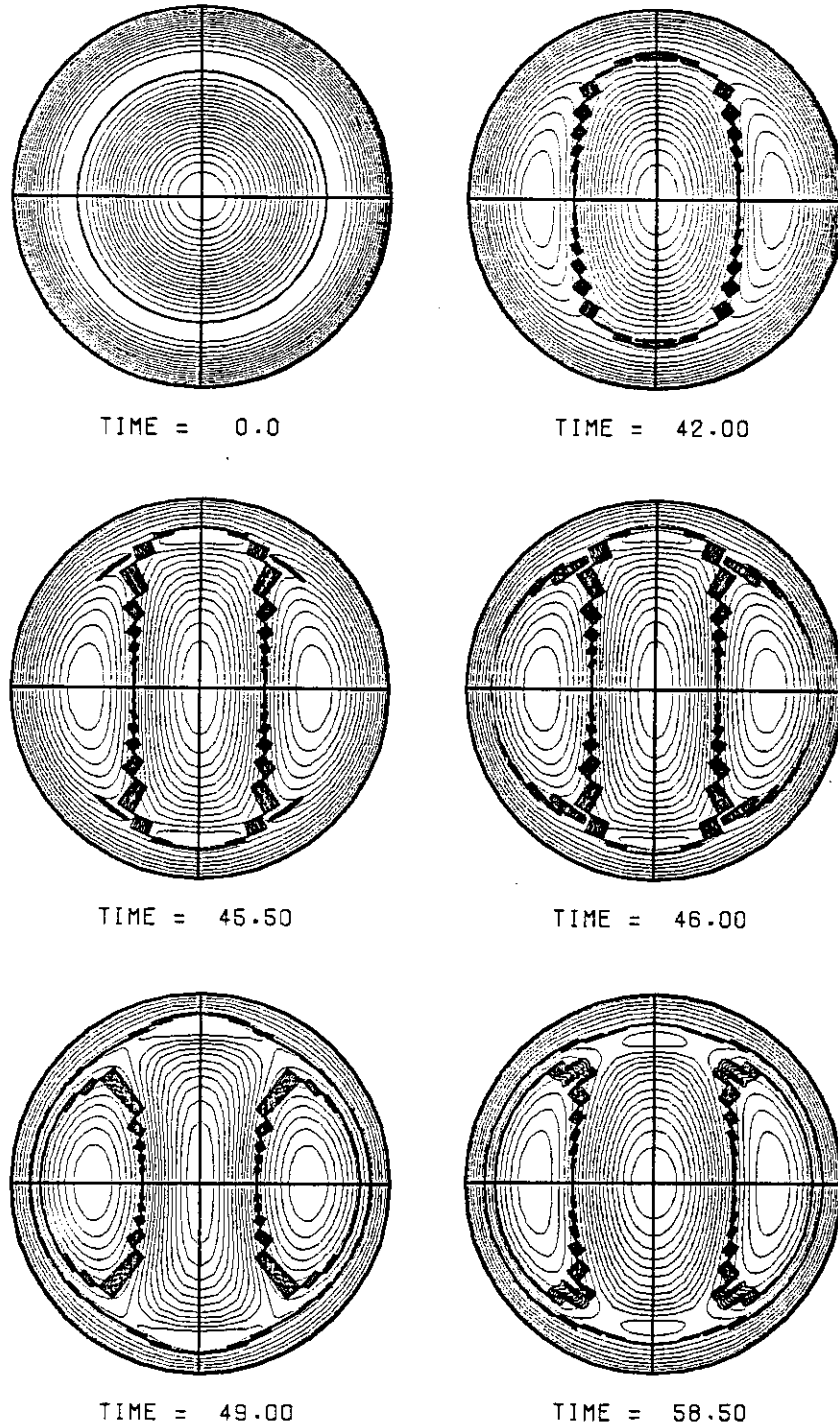


FIG.4 Time evolutions of ψ -contours and plasma surface for current profile; $J(r)=J(0)(1-(r/a)^{6.14})^2$ with $q_{a0}=1.85$. Ratio, $q_0/q_a|_{t=0}$, corresponds to calculation of Ref. [8].

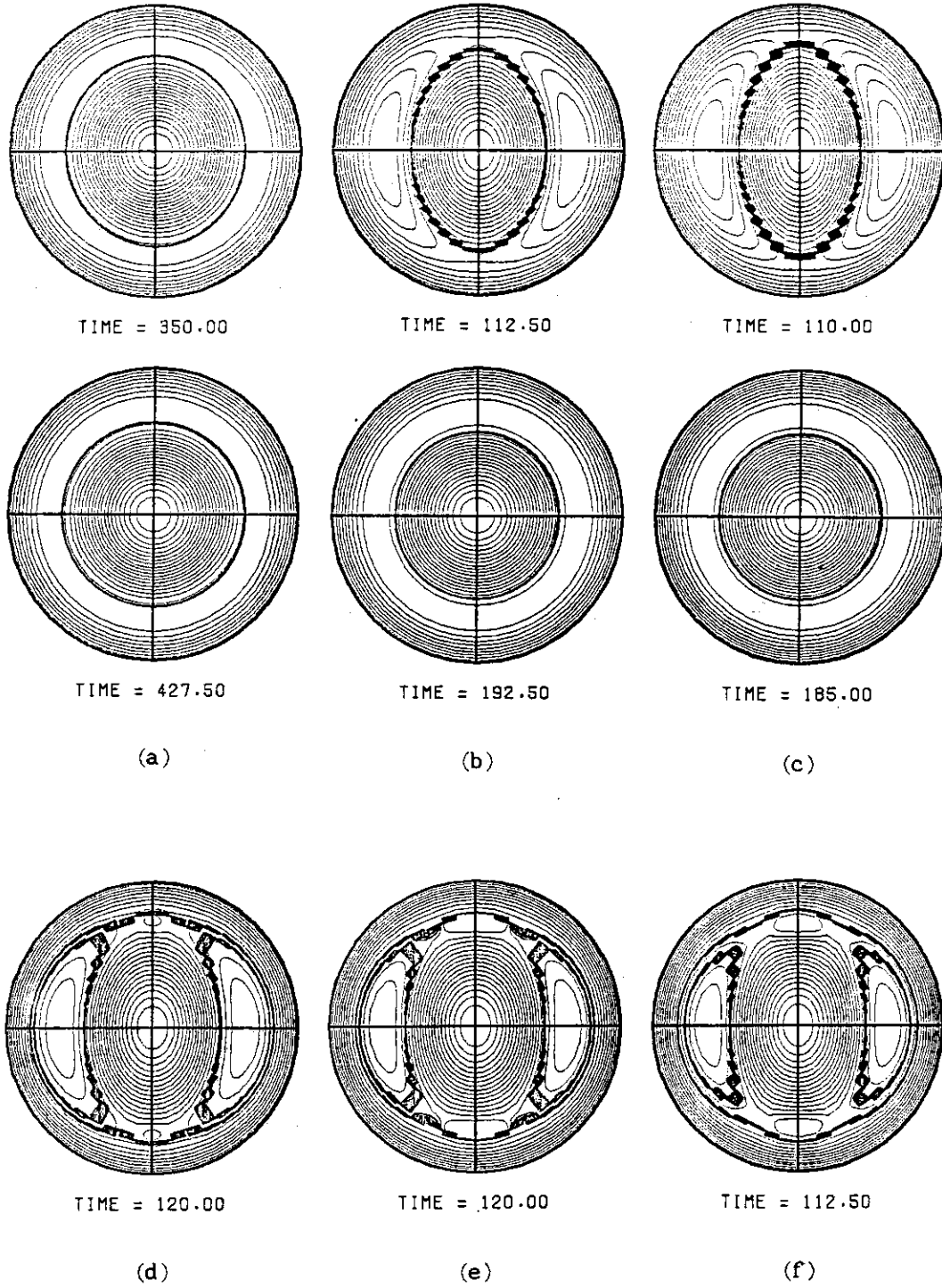


FIG.5 Final states of Ψ -contours and plasma surface for current profile; $J(r)=J(0)(1-(r/a)^{3.56})^2$ with various q_{a0} values, (a) $q_{a0}=1.75$, (b) $q_{a0}=1.8$, (c) $q_{a0}=1.85$, (d) $q_{a0}=1.9$, (e) $q_{a0}=1.95$ and (f) $q_{a0}=2.0$. Elliptic deformation of plasma surface at about maximum magnetic energy state for cases of plasma shrinkage, (a)~(c), are also shown.

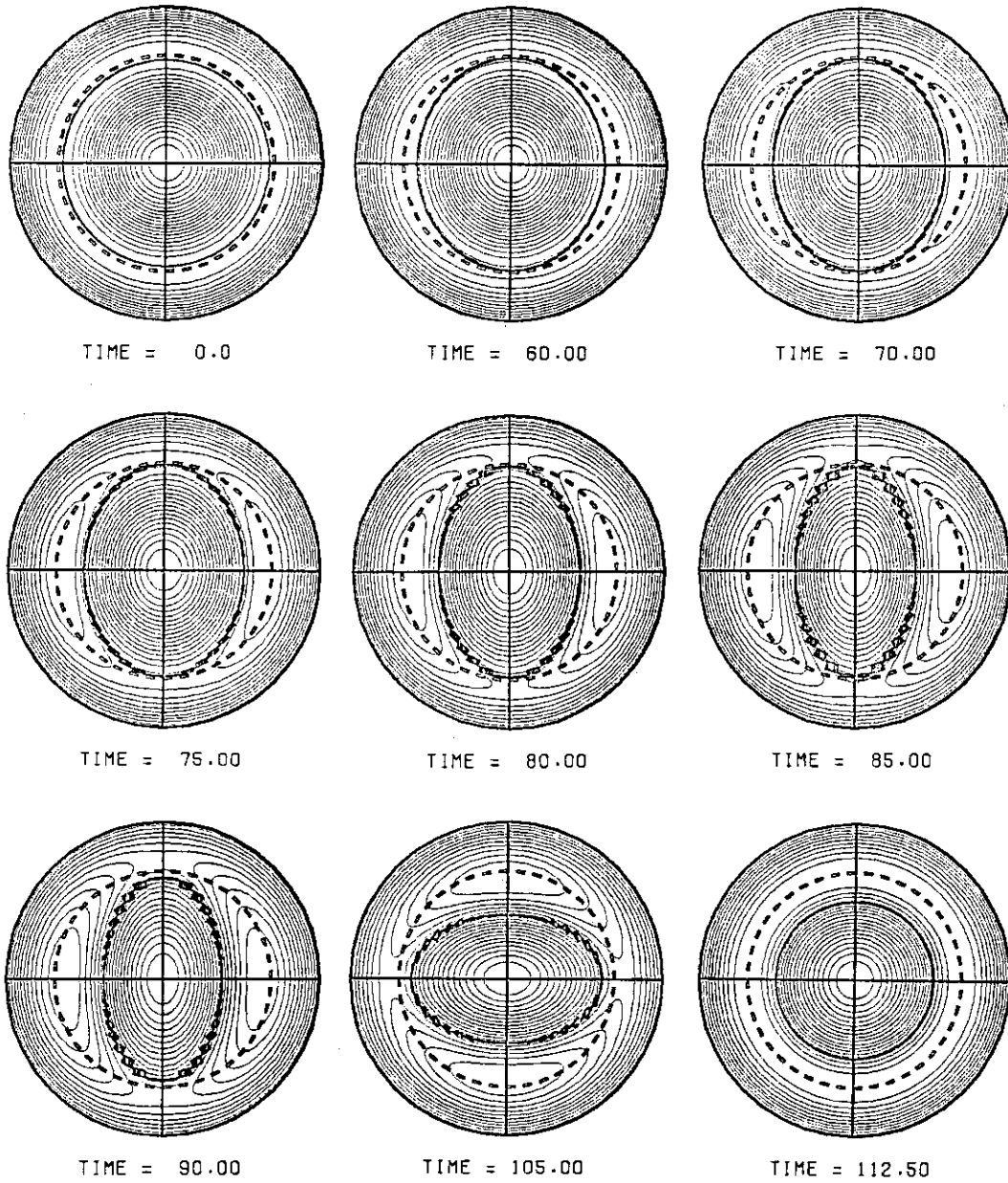


FIG.6 Time evolutions of Ψ -contour and plasma surface for $q_{a0}=1.85$. Limiter is placed at $r=1.03a_0$. The plasma touches limiter at $t\approx 55.0$ and is detached from it at $t\approx 87.0$.

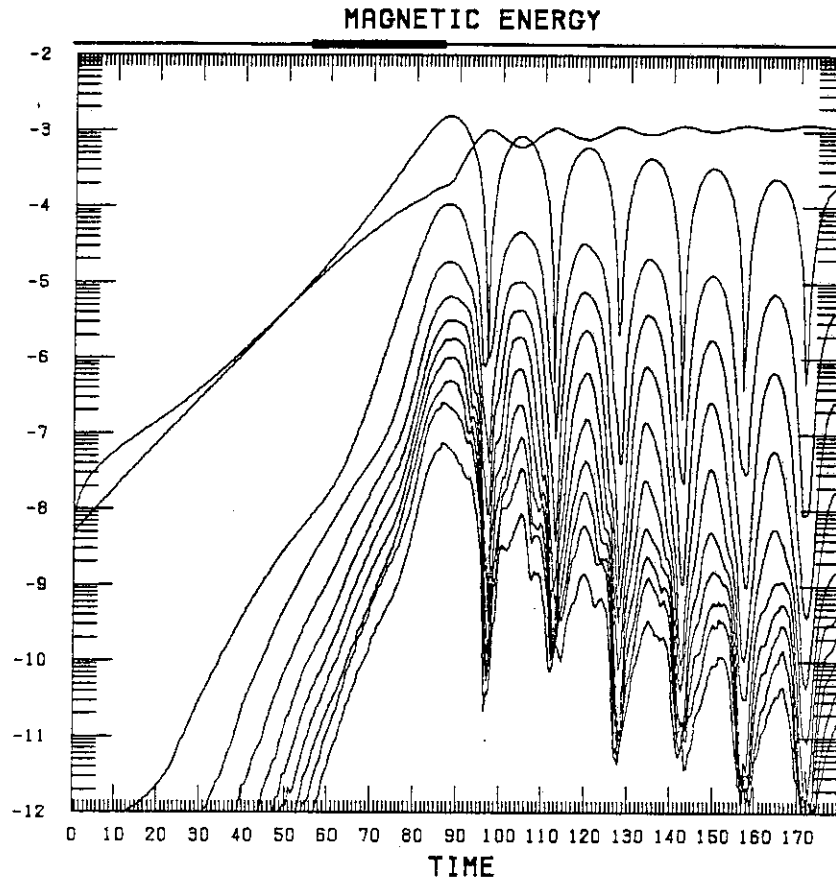


FIG.7 Time evolutions of magnetic energy of each mode for $q_{a0}=1.85$ with limiter. Bold line, shown upper side of figure, denotes the time duration when the plasma contacts with limiter. Mode numbers are $m/n=0/0, 2/1, 4/2, \dots, 20/10$ from top to bottom, respectively.

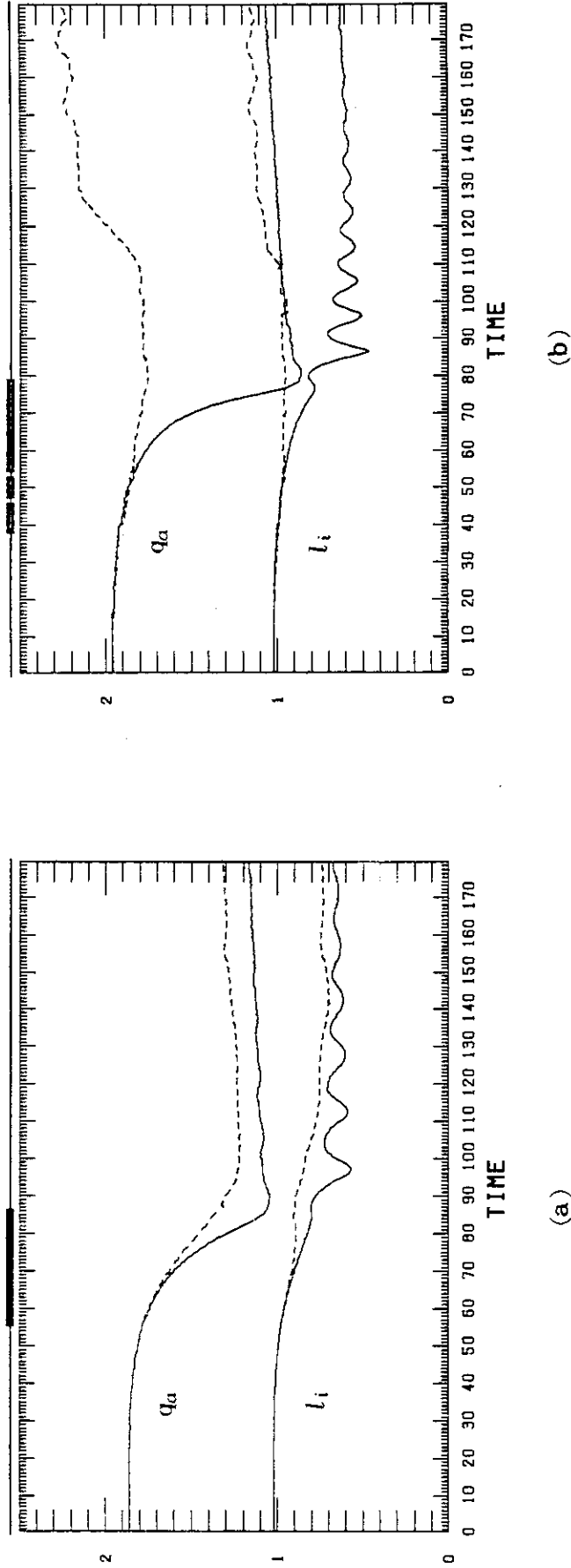


FIG.8 Time evolutions of q_a and internal inductance l_i for (a) $q_{a0}=1.85$ and (b) $q_{a0}=1.95$. Results of calculation with and without limiter are shown by solid and broken curves, respectively. Bold line, shown upper side of figure, denotes the time duration when the plasma contacts with limiter.

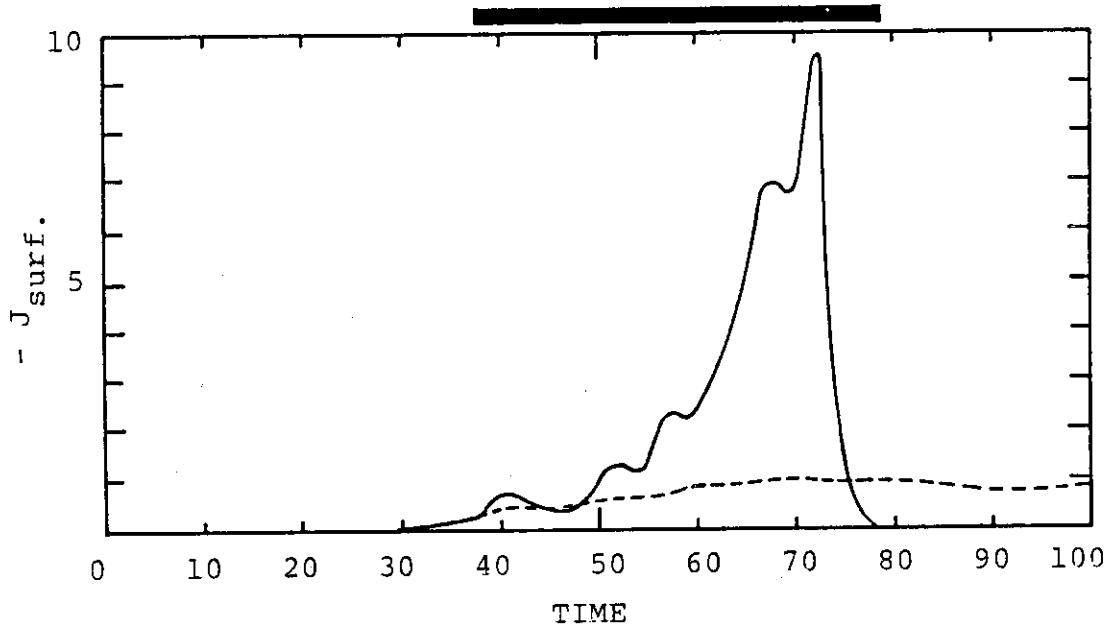


FIG.9 Time evolutions of maximum value of negative surface-current near top or bottom of plasma poloidal plane in Fig.6. This is the same calculation as in Fig.8(b). Bold line, shown upper side of figure, denote the time duration when the plasma contacts with limiter. Broken line denotes result without limiter.

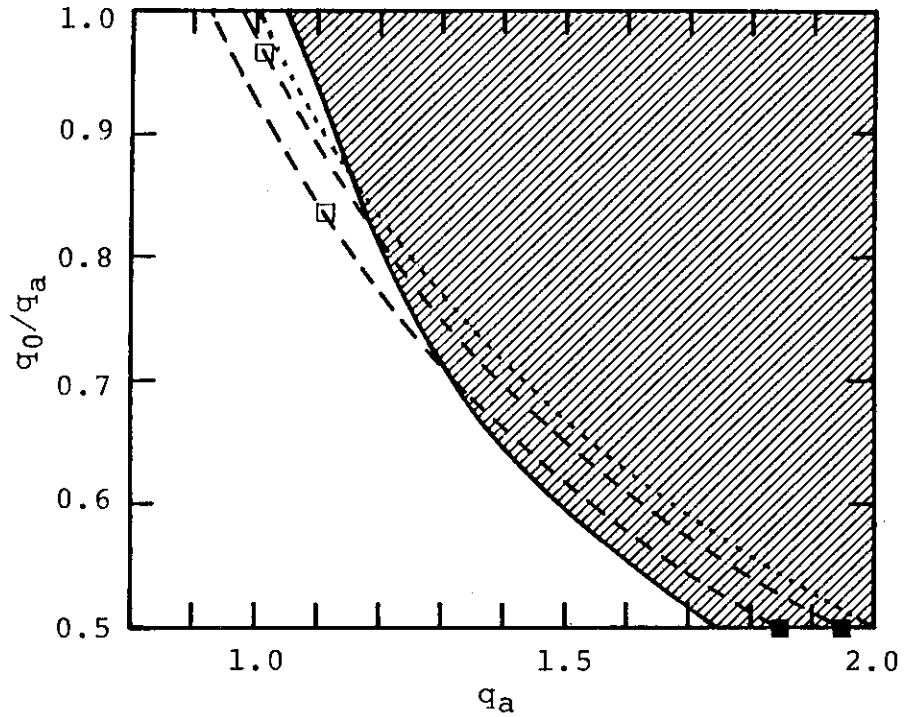


FIG.10 Stability diagram of $m/n=2/1$ free-boundary kink mode for approximated current density profile to that realized in nonlinear calculations. Hatched region denotes unstable one, and two broken lines of trajectory correspond to nonlinear calculations with limiter for $q_{a0}=1.85$ and $q_{a0}=1.95$. Black and open squares denote start and final positions, respectively. Trajectory of $q_{a0}=2.0$ ($q_0=1.0$) is shown by dotted line. Plasma radius is determined from condition of constant total current, i.e., $a=a_0\sqrt{q_a/q_{a0}}$ with $a_0/b=0.66$.

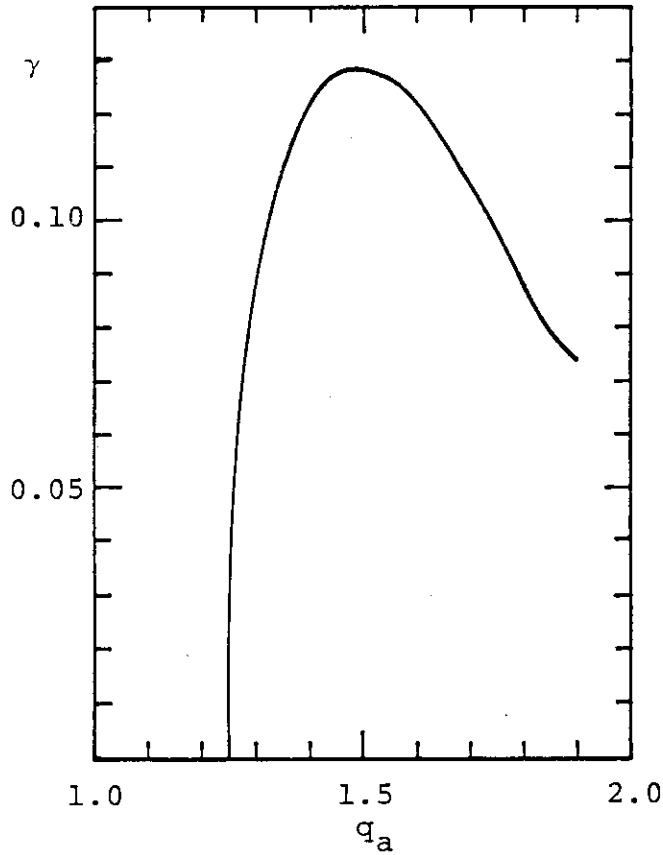


FIG.11 Change of linear growth rates along trajectory for $q_{a0} = 1.90$ with constant q_0 , unstable region of which is shown in Fig.10. Current density profiles are determined from following formula,

$$j(r) = j_0 \left\{ \left(1 - (r/a_0)^{3.56} \right)^2 + \lambda \exp(-2((r-a+\mu)/\nu)^2) \right\} \left\{ 1 - (r/a)^\nu \right\}^2.$$

Height of skin current, λ , is determined from condition of constant total current for fixed position of skin current, $\mu = 0.1a_0$, and width of that, $\nu = 0.05a_0$. Value of ν , which denotes current gradient near plasma surface, is chosen to be several ten.